

Configuration interaction study on low-lying states of AlCl molecule

Xiao-Ying Ren(任笑影), Zhi-Yu Xiao(肖志宇), Yong Liu(刘勇), Bing Yan(闫冰)

Citation: Chin. Phys. B, 2021, 30 (**5**): 053101. DOI: 10.1088/1674-1056/abd46a
Journal homepage: http://cpb.iphy.ac.cn; http://iopscience.iop.org/cpb

What follows is a list of articles you may be interested in

Theoretical insights into photochemical ESITP process for novel DMP-HBT-py compound

Guang Yang(杨光)†, Kaifeng Chen(陈凯锋), Gang Wang(王岗), and Dapeng Yang(杨大鹏)
Chin. Phys. B, 2020, 29 (**10**): 103103. DOI: 10.1088/1674-1056/aba9bb

Exploration and elaboration of photo-induced proton transfer dynamical mechanism for novel 2-[1,3]dithian-2-yl-6-(7aH-indol-2-yl)-phenol sensor

Lei Xu(许磊), Tian-Jie Zhang(张天杰), Qiao-Li Zhang(张巧丽), Da-Peng Yang(杨大鹏)
Chin. Phys. B, 2020, 29 (**5**): 053102. DOI: 10.1088/1674-1056/ab8208

Vibronic spectra of aluminium monochloride relevant to circumstellar molecule

Jian-Gang Xu(徐建刚), Cong-Ying Zhang(张聪颖), Yun-Guang Zhang(张云光)
Chin. Phys. B, 2020, 29 (**3**): 033102. DOI: 10.1088/1674-1056/ab6c46

The substituent effect on the excited state intramolecular proton transfer of 3-hydroxychromone

Yuzhi Song(宋玉志), Songsong Liu(刘松松), Jiajun Lu(陆佳骏), Hui Zhang(张慧), Changzhe Zhang(张常哲), Jun Du(杜军)
Chin. Phys. B, 2019, 28 (**9**): 093102. DOI: 10.1088/1674-1056/ab3434

Accurate spectroscopic constants of the lowest two electronic states in S_2 molecule with explicitly correlated method

Changli Wei(魏长立), Xiaomei Zhang(张晓美), Dajun Ding(丁大军), Bing Yan(闫冰)
Chin. Phys. B, 2016, 25 (**1**): 013102. DOI: 10.1088/1674-1056/25/1/013102

Configuration interaction study on low-lying states of AlCl molecule*

Xiao-Ying Ren(任笑影), Zhi-Yu Xiao(肖志宇), Yong Liu(刘勇), and Bing Yan(闫冰)†

Institute of Atomic and Molecular Physics, Jilin University, Changchun 130012, *China*

(Received 20 October 2020; revised manuscript received 7 December 2020; accepted manuscript online 17 December 2020)

High-level *ab initio* calculations of the Λ–S states for aluminum monoiodide (AlCl) molecule are performed by utilizing the explicitly correlated multireference configuration interaction (MRCI-F12) method. The Davidson correction and scalar relativistic correction are investigated in the calculations. Based on the calculation by the MRCI-F12 method, the spin–orbit coupling (SOC) effect is investigated with the state-interacting technique. The adiabatic potential energy curves (PECs) of the 13 Λ–S states and 24 Ω states are calculated. The spectroscopic constants of bound states are determined, which are in accordance with the results of the available experimental and theoretical studies. Finally, the transition properties of $0^+(2)$–$X0^+$, $1(1)$–$X0^+$, and $1(2)$–$X0^+$ transitions are predicted, including the transition dipole moments (TDMs), Franck–Condon factors (FCFs), and the spontaneous radiative lifetimes.

Keywords: AlCl molecule, MRCI-F12, potential energy curves, spin–orbit coupling

PACS: 31.15.A–, 31.15.aj, 31.50.Bc, 31.50.Df **DOI:** 10.1088/1674-1056/abd46a

1. Introduction

Some aluminum halide molecules (AlX, X = F, Cl, Br, I) have been detected in the astrophysical environment[1] and are also easy to generate chemiluminescent reactions in the gas phase through high temperature pyrolysis.[2] In recent years, monochloride has received more and more attention.[3–6] In order to further understand the physical and chemical processes involving these molecules, the characteristics of their electronic states including spectroscopic constants and transition properties are extremely important. Aluminum halides have also aroused the increasing research interest due to their potential applications in molecular laser cooling. In theory, Wells and Lane[4] have performed *ab initio* studies of the electronic states of AlH and AlF, showing that the $A^1\Pi$–$X^1\Sigma^+$ transition of two molecules may be strong candidates for laser cooling. For AlCl, the $A^1\Pi_1$–$X^1\Sigma^+_{0+}$ transition is also a possible candidate for laser cooling.[7]

For AlCl molecule, many experimental and theoretical studies have been performed previously. The spectrum of AlCl molecule focused mainly on the ground state $X^1\Sigma^+$ and several low-lying states. Hedderich *et al.*[8] discovered the high-resolution emission spectrum of AlCl and found a rotational transition occurring in a range of 5 mm–7 mm. Lanhoff *et al.*[9] predicted the spectroscopic constants of the ground state and excited states with energy up to 61000 cm^{-1} by high-level *ab initio* calculations. In 2011, Wells and Lane[4] observed the transition of $AlCl_3$ in the discharge experiment of AlCl and conducted vibration analysis. In 1951, Sharma[7] found that the wavelength band of 415.4 nm–397 nm was similar to the Cameron band of CO, which was caused by the transition from the first excited state of AlCl to the ground state. Dearden *et al.*[10] used 332 nm–570 nm laser resonance enhancement photoionization spectroscopy to study the highly excited states of 24000 cm^{-1}–60000 cm^{-1} and obtained spectroscopic constants for seven new states of AlCl. In addition, Saksena *et al.*[11] observed the $a^3\Pi$–$X^1\Sigma^+$ transition of the AlCl molecule at a high resolution and determined the rotation constant of the $a^3\Pi$ state. Mahieu *et al.*[12] also studied the $A^1\Pi$–$X^1\Sigma^+$ system of AlCl and obtained the accurate rotational constants and vibrational constants of these two states, and discussed the predissociation of the $A^1\Pi$ state at the $v' = 10$ vibration energy level. In 1987, Rogowsiu and Fontijn[13] determined the radiative lifetime of the AlCl $A^1\Pi$ state ($\tau = 6.4$ ns) by using laser-induced fluorescence technique. In theory, Brites and Hochlaf [14] calculated the potential energy curves of electronic states for AlCl and its cationic species $AlCl^+$ and $AlCl^{2+}$ at the MRCI level, and derived a set of accurate spectroscopic constants. Langhoff *et al.*[9] computed spectroscopic constants for the lowest six singlet states and the lowest five triplet states of AlCl by the MRCI+Q method. And the lifetime of the $v' = 0$ level of the $A^1\Pi$ state for AlCl is calculated to be 5.2 ns. The latest *ab initio* computation[3] was reported in 2016, in which the potential energy curves, permanent dipole moments, and transition dipole moments for the $X^1\Sigma^+$, $a^3\Pi$, and $A^1\Pi$ states were studied by the MRCI+Q method with the ACVQZ basis set.[15]

Although AlCl molecule has been studied for a long time, our knowledge of the excited states of the molecule, especially

*Project supported by the National Key Research and Development Program of China (Grant No. 2017YFA0403300), the National Natural Science Foundation of China (Grant Nos. 11874177, 11874179, and 11574114), the Natural Science Foundation of Jilin Province, China (Grant No. 20180101289JC), and the High Performance Computing Center of Jilin University and High Performance Computing Cluster Tiger@IAMP (Theoretical Simulation Laboratory of Generalized Atomic, Molecular, and Energy Researches at Institute of Atomic and Molecular Physics).

†Corresponding author. E-mail: yanbing@jlu.edu.cn

© 2021 Chinese Physical Society and IOP Publishing Ltd

the complete picture of spin–orbit coupling in electronic excited states, is far from enough. In this paper, we perform the explicitly correlated multireference configuration interaction plus Davidson correction (MRCI-F12+Q) method to calculate the PECs of the 13 Λ–S states of the AlCl molecule. The scalar relativistic (SR) correction is considered in this work. The SOC interactions between the Λ–S states are evaluated by the SO matrix elements. After considering the SOC effect, 13 Λ–S states split into 24 Ω states. The spectroscopic constants of Ω states are evaluated. The permanent dipole moments (PDMs), transition dipole moments (TDMs), Franck–Condon factors (FCFs), and the radiative lifetimes of several lowest transitions are also predicted.

2. Computational methods

For AlCl molecule, we perform 71 single point energy calculations for each state with the internuclear distance in a range of R value of 0.8 Å–8.5 Å to construct the potential energy curves. The high-level *ab initio* calculations on the electronic structure are performed with the quantum chemistry MOLPRO 2012 program package.[16] The symmetric point group of AlCl is $C_{\infty v}$. The C_{2v} point group is selected for the AlCl electronic structure calculation. The C_{2v} point group has an irreducible representation of $A_1/B_1/B_2/A_2$, and the corresponding relationships with the $C_{\infty v}$ point group are $\Sigma^+ = A_1$, $\Pi = B_1 + B_2$, $\Delta = A_1 + A_2$, and $\Sigma^- = A_2$, respectively. A total of 13 Λ–S states corresponding to the two lowest dissociation limits, neutral Al(^{2}P$_u$)+Cl(^{2}P$_u$) and ionic pair Al$^+$(^{1}S)+Cl(^{1}S), are investigated in this work. Firstly, the restricted Hartree–Fock (HF) method is used to obtain the single-configuration wavefunction of the ground state for the AlCl molecule; then the state-averaged complete active space self-consistent field (SACASSCF)[17,18] is used. In the SA-CASSCF computations, we involve a total of 13 electronic states including three $^1\Sigma^+$, two $^1\Pi$, one $^1\Delta$, one $^1\Sigma$, two $^3\Sigma^+$, two $^1\Pi$, one $^3\Delta$, and one $^3\Sigma$ states. The MRCI-F12 method is utilized to estimate the dynamical correlations. At the same time, the Davidson[19] correction (+Q) balances the size-consistency error of multireference method. Moreover, the calculation is extended to including the scalar relativistic effect by means of an electronic third-order Douglas-Kroll[20–22] integral.The basis set chosen in MRCI-F12 calculation is the cc-CVQZ-F12 for Al and Cl atoms.

In the following calculations, the influence of the SOC effect on the MRCI-F12 calculation level is considered. The SOC matrix element[23,24] is dealt with by the state-interacting technique via Breit–Pauli operator.[25] The off-diagonal spin–orbit matrix elements are calculated at the MRCI-F12 level, while the diagonal spin–orbit matrix elements are substituted with the MRCI-F12+Q energy. The SOC effect makes the 13 Λ–S electronic states split into 24 Ω states. The PECs of the 13 Λ–S states and 24 Ω states draw and meet the rule of avoided crossing. On the basis of the PECs in Λ–S and Ω states, the spectroscopic constants of the bound states can be determined by solving the numerical solution of the one-dimensional nuclear Schrödinger equation through the Level program,[26] including the excitation energy T_e, the equilibrium internuclear distance R_e, the vibration constant ω_e and $\omega_e x_e$, and the harmonic vibration constant B_e. The dissociation energy D_e is obtained by subtracting the energy at R_e from the energy at a large interval. The transition properties and the spin–orbit matrix elements of several electronic states of AlCl molecule are calculated. The permanent dipole moments (PDMs), the transition dipole moment (TDMs), and the Franck–Condon factors (FCFs) are also calculated at the MRCI-F12 level. According to the calculated TDMs and FCFs, we predict the radiative lifetimes of several lowest transitions.

3. Results and discussion

3.1. Potential energy curves and spectroscopic constants of 13 Λ–S states

We calculate 13 Λ–S states of AlCl molecule by the method of MRCI-F12+Q, including 7 singlet states and 6 triplet states. Figure 1 displays the potential energy curves of 13 Λ–S states of AlCl molecule. These states correspond to two dissociation limits of Al(^{2}P$_u$)+Cl(^{2}P$_u$) and Al$^+$(^{1}S)+Cl$^-$(^{1}S) and are listed in Table 1. As shown in Table 1, except for the $^1\Sigma^+$ state, which is associated with the ion-pair dissociation limit Al$^+$(^{1}S)+Cl^{-1}(^{1}S), the other Λ–S states correspond to the same neutral atomic dissociation limit Al(^{2}P$_u$)+Cl(^{2}P$_u$). The energy interval between the two atomic limits is computed at the internuclear distance $R = 6$ Å with the inclusion of Coulomb compensation for the energy.

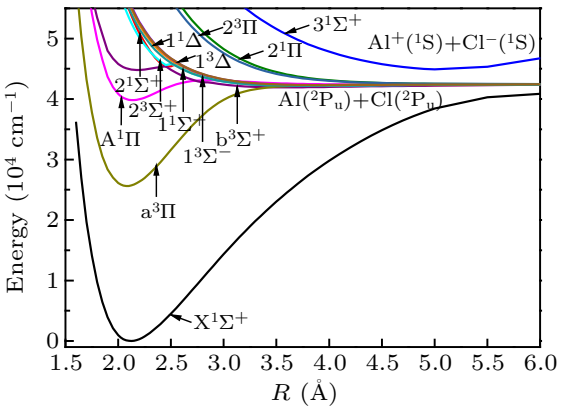


Fig. 1. PECs of Λ–S states for AlCl.

From Fig. 1, we can see that the two singlet states X$^1\Sigma^+$ and A$^1\Pi$ and one triplet state a$^3\Pi$ are typical bound states, while the other states are repulsive states or quasi-bound states. It can be seen from Fig. 1 that there is an avoided crossing point between b$^3\Sigma^+$ and 2$^3\Sigma^+$ states at internuclear distance $R = 2.4$ Å, which results in the formation of a potential well in the 2$^3\Sigma^+$ state and a potential barrier in the b$^3\Sigma^+$ state.

Table 1. Dissociation relationships of Λ–S states of AlCl.

Atomic state	Λ–S states	Energy (cm^{-1})	
		Calc.	Expt.[a]
$Al(^2P_u)+Cl(^2P_u)$	$X^1\Sigma^+$, $2^1\Sigma^+$, $A^1\Pi$, $2^1\Pi$, $a^3\Pi$, $1^1\Delta$, $1^1\Sigma^-$, $b^3\Sigma^+$, $2^3\Sigma^+$, $2^3\Pi$, $1^3\Delta$, $1^3\Sigma^-$	0	0
$Al^+(^1S)+Cl^-(^1S)$	$3^1\Sigma^+$	19354	19109

[a]Refs. [27–29].

Table 2. Computed and experimental spectroscopic constants of low-lying Λ–S states of AlCl.

State	Reference	Method	T_e (cm^{-1})	R_e (Å)	ω_e (cm^{-1})	$\omega_e x_e$ (cm^{-1})	B_e (cm^{-1})	D_e (eV)
$X^1\Sigma^+$	this work	MRCI-F12/CVQZ		2.1246	489.7	2.053	0.2452	5.54
	this work	$\Delta+Q$		+0.0012	–1.9	–0.026	–0.003	+0.03
	this work	ΔSR		–0.004	–0.5	–0.009	+0.0001	–0.10
	this work	MRCI-F12/CVQZ+Q+DK		2.1254	487.1	2.24	0.2450	5.36
	Calc.[13]	MRCI+Q/cc-pwCV5Z		2.1400	484.5	6.47	0.2418	5.25±0.1(D)
	Calc.[8]	MRCI+Q		2.1460	467.			
		MRCI		2.149	472.			
	Calc.[3]	MRCI+Q		2.1374	478.1		0.2408	5.21
	Expt.[11]				481.4	2.037		
	Expt.[31]			2.130	481.7	2.07	0.2439	5.25±0.01(D)
	Expt.[9]				481.0			
	Expt.[8]			2.130	481.8	2.10		
	Expt.[32]							5.16±0.04
	Expt.[28]			2.1301	481.3		0.2439	
	Expt.[33]				480.2			
$a^3\Pi$	this work	MRCI-F12/CVQZ	22958	2.0877	540.6	2.199	0.254	2.45
	this work	$\Delta+Q$	–1010	–0.0021	–3.8	+0.035	–0.0006	–0.05
	this work	ΔSR	–154	–0.0007	–0.7	+0.014	+0.0001	–0.03
	this work	MRCI-F12/CVQZ+Q+DK	24120	2.0895	536.0	2.245	0.2536	2.37
	Calc.[13]	MRCI+Q/cc-pwCV5Z		2.107	519.1	0.52	0.2494	
	Calc.[8]	MRCI+Q	24194	2.114	519.0			
		MRCI	23819	2.110	530.0			
	Calc.[3]	MRCI+Q	23960	2.1050	525.7		0.2483	2.25
	Expt.[31]		24793		520.0		0.2524	
	Expt.[12]						0.2534	
	Expt.[7]			2.1000	524.4	2.175	0.250	
$A^1\Pi$	this work	MRCI-F12/CVQZ	39693	2.1231	450.4	6.886	0.2455	0.49
	this work	$\Delta+Q$	–218	–0.0064	+21	–1.576	0.2441	+0.06
	this work	ΔSR	–83	+0.0022	–7	–0.414	0.245	–0.02
	this work	MRCI-F12/CVQZ+Q+DK	39561	2.131	456.7	7.106	–0.2437	–0.53
	Calc.[13]	MRCI+Q/cc-pwCV5Z		2.132	453.	8.03	0.2435	
	Calc.[8]	MRCI+Q	38453	2.152	449.0			
		MRCI	39630	2.138	464.			
	Calc.[3]	MRCI+Q	38224	2.133	454.2		0.2397	0.54
	Expt.[12]		38268	2.1237	441.6	2.81	0.2443	
	Expt.[10]		38236		429.0			
	Expt.[31]				450.0		0.2454	
	Expt.[33]				452.9			

[a]The value was calculated by the equation $B_e = h/(8\pi^2\mu R_e^2)$.

The spectroscopic constants of these three states are calculated by the MRCI-F12 method, and those results obtained from previous experimental and theoretical studies are listed in Table 2 for comparison. The ground state $X^1\Sigma^+$ of the AlCl molecule is characterized mainly by the closed-shell electronic configuration $7\sigma^2 8\sigma^2 9\sigma^2 3\pi^4$ (85.043%) at R_e. The deviations of R_e, ω_e, and D_e calculated by MRCI-F12/CVQZ+Q+DK from the previous experimental value,[25,30] are 0.0046 Å, 6 cm^{-1}, and 0.11 eV, respectively. Therefore, it indicates that the Davidson correction is still important for the MRCI-F12 approach to solve the size-extensivity problem. For the first excited state $a^3\Pi$, the wavefunction of $a^3\Pi$ is mainly described by the electronic configuration $7\sigma^2 8\sigma^2 9\sigma^\alpha 3\pi^4 4\pi^\alpha$ (86.177%). The Davidson correction and SR correction contribute about 1162 cm^{-1} to the value of T_e, the previous calculated R_e values by various methods are similar and our calculation is about 2.09 Å, which is somewhat smaller than the experimental value of 2.1 Å. At

the same time, the differences among ω_e values obtained by different methods are also small. To the best of our knowledge, no experimental value for D_e of $a^3\Pi$ state is found. The D_e of the $a^3\Pi$ state is evaluated to be 2.37 eV, which is in good agreement with the theoretical result of 2.25 eV.[3] For the $A^1\Pi$ state, the wavefunction is described mainly by the electronic configuration $7\sigma^2 8\sigma^2 9\sigma^\alpha 3\pi^4 4\pi^\beta$ (78.954%). The R_e, ω_e, and D_e values for the $A^1\Pi$ state are calculated to be 2.131 Å, 456.7 cm^{-1}, and 0.53 eV, respectively, which are in good agreement with the previous theoretical values.[3] While all the computed values of T_e deviate from the experimental values by larger than 500 cm^{-1}.[10]

Figure 2 shows the permanent dipole moments (PDMs) of the 13 Λ–S states of AlCl molecule. For clarity, the PDMs of singlet states and triplet states are represented in Figs. 2(a) and 2(b), respectively. The PDMs of $X^1\Sigma^+$, $a^3\Pi$, and $A^1\Pi$ states for AlCl molecule have been calculated previously.[3] As shown in Fig. 2, all the calculated PDMs at a large internuclear distance are almost zero a.u. (atomic unit) with the exception of the $3^1\Sigma^+$ state. This is because the center of positive charges with the position vector λ is set to be at zero, which is corresponding to the dissociation limit of neutral atom. The variation of PDM can reflect the ionic characteristics of these states. The PDM of $3^1\Sigma^+$ state is negative and becomes linearly-dependent R when R is larger than 6.0 Å. This indicates that the dissociation limit of the $3^1\Sigma^+$ state comes from ion-pair $Al^+(^1S)$+$Cl(^1S)$. The PDMs of $X^1\Sigma^+$ and $a^3\Pi$ states have negative peaks with values of −4.26 a.u. and −1.04 a.u. at $R = 4.4$ Å and $R = 2.9$ Å, respectively.

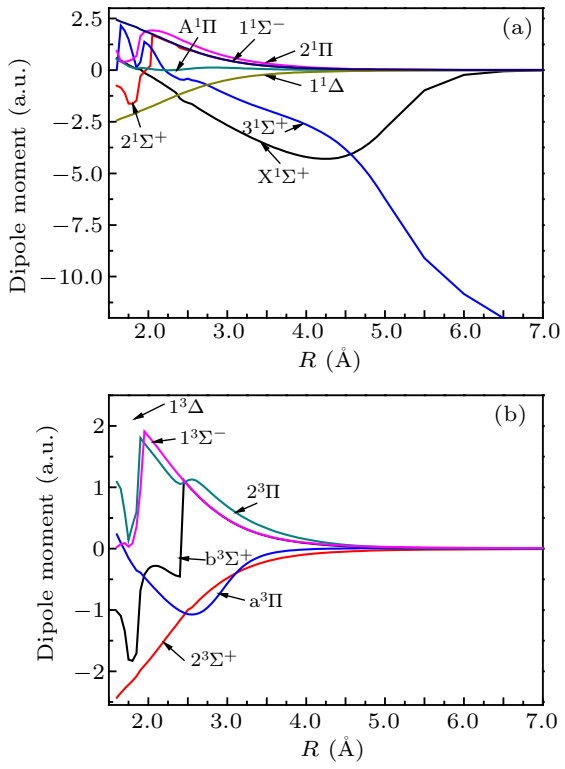


Fig. 2. Permanent dipole moments of Λ–S states for AlCl molecule.

3.2. Spin–orbit coupling of the Λ–S states

The SOC effect has a significant effect on the AlCl molecule and cannot be ignored. The SOC effect leads the energy level to be split and the Λ–S states to be mixed with a common Ω. To clarify the strong interactions between the electronic states of AlCl, we calculate the values of SOC matrix element $|H_{so}|$. The calculated SO matrix elements are plotted in Fig. 3 as a function of internuclear distance. The symbols of computed SO matrix elements are listed in Table 3. From Fig. 3, we can see that $|H_{so}|$ is in a range of 0 cm^{-1}–160 cm^{-1}. The PECs of $A^1\Pi$ state and $b^3\Sigma^+$ state have a crossing phenomenon at $R = 2.7$ Å. As illustrated in Figs. 1 and 3, at the crossing point between $A^1\Pi$ and $b^3\Sigma^+$ states, the H_{so} value is −138 cm^{-1}; and near the crossing point located is the $v' = 9$ vibrational level of $A^1\Pi$ high ($v' = 9$). Therefore, the predissociation of the $A^1\Pi$ ($v' = 9$) state can occur through the SO coupling with $b^3\Sigma^+$ state.

Table 3. SO matrix elements of Λ–S state.

Spin–orbit matrix elements	
$SO_1 = -i\langle a^3\Pi\|H_{so}\|1^3\Delta\rangle_x$	$SO_6 = -i\langle A^1\Pi\|H_{so}\|1^3\Sigma^-\rangle_x$
$SO_2 = -i\langle a^3\Pi\|H_{so}\|1^3\Sigma^-\rangle_x$	$SO_7 = -i\langle A^1\Pi\|H_{so}\|b^3\Sigma^+\rangle_y$
$SO_3 = -i\langle a^3\Pi\|H_{so}\|a^3\Pi\|_z$	$SO_8 = -i\langle A^1\Pi\|H_{so}\|2^3\Sigma^+\rangle_y$
$SO_4 = -i\langle a^3\Pi\|H_{so}\|2^3\Pi\|_z$	$SO_9 = -i\langle A^1\Pi\|H_{so}\|a^3\Pi\rangle_z$
$SO_5 = -i\langle A^1\Pi\|H_{so}\|1^3\Delta\rangle_x$	$SO_{10} = -i\langle A^1\Pi\|H_{so}\|2^3\Pi\rangle_z$

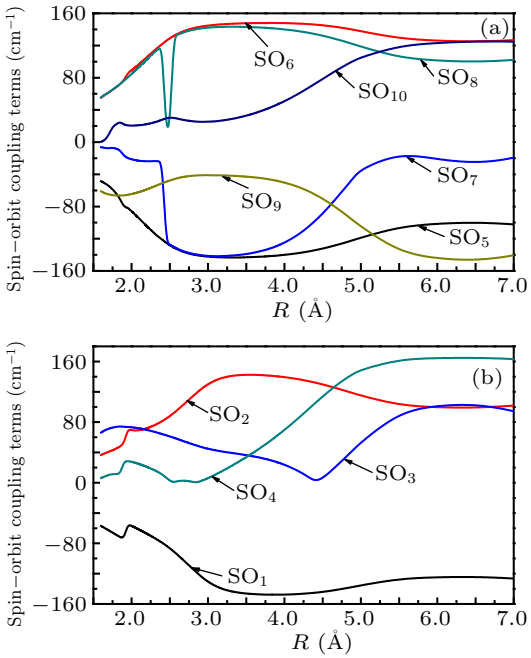


Fig. 3. Spin–orbit matrix elements of several Λ–S states, with definition of the SO_i symbols in Table 3.

3.3. PECs and spectroscopic constants of Ω states

Taking the SOC effect into account, the two dissociation limits split into five dissociation limits. The 13 Λ–S states split into 24 Ω states, including six states of $\Omega = 0^+$, five states of $\Omega = 0^-$, eight states of $\Omega = 1$, four states of $\Omega = 2$, and one state of $\Omega = 3$. The detailed dissociation relationships

of Ω states and the corresponding energy splitting are illustrated in Table 4. The computed energy intervals of $Al(^2P_{3/2u})$ –$Al(^2P_{1/2u})$ and $Cl(^2P_{1/2u})$–$Cl(^2P_{3/2u})$ are 120 cm^{-1} and 875 cm^{-1}, which are in excellent agreement with the experimental values[27–29] of 112 cm^{-1} and 882 cm^{-1}, respectively. As for the ion-pair limit $Al^+(^1S_{0g})$+$Cl^-(^1S_{0g})$, we estimate the $1/R$ Coulomb compensation from $R = 6$ Å to infinite distance. The computational value of the $Al^+(^1S_{0g})$+$Cl(^1S_{0g})$ is 245 cm^{-1} higher than experimental result of 19109 cm^{-1}, which maybe result from the fact that it is not far enough to treat the AlCl molecule as two independent ions at $R = 6$ Å.

In Fig. 4, we show the calculated PECs of the 24 Ω states of AlCl. The potential energy curves are plotted following the avoided crossing rule of states with the same symmetry. Taking the SOC effect into account, there are strong interactions and a number of avoided crossings between these Ω states, especially in the ultraviolet region. There are three avoided crossing points located at $R = 2.2$ Å ($\Omega = 0^+$), $R = 2.45$ Å ($\Omega = 0$), and $R = 2.4$ Å ($\Omega = 1$), respectively, which are shown in Fig. 4. The state $\Omega = 3$ is purely generated from the $1^3\Delta$ state, therefore, the shape of the PEC for $\Omega = 3$ is similar to that of the corresponding Λ–S state. For the remaining Ω states, the shapes of the PECs are very complex in an energy range of 37000 cm^{-1}–47000 cm^{-1}. Some of them (*e.g.* $0^+(6)$, $0^+(3)$, $0^-(4)$, $0^-(2)$, 1(3), and 1(6)) have two or more shallow potential wells due to the SOC effect.

Table 4. Dissociation relationship of the Ω states of AlCl.

Atomic state	Ω states	Energy (cm^{-1})	
		Calc.	Expt.[a]
$Al(^2P_{1/2u})$+$Cl(^2P_{3/2u})$	$X0^+$, $0^-(1)$, 1(1), 1(2), 2(1)	0	0
$Al(^2P_{3/2u})$+$Cl(^2P_{3/2u})$	$0^+(2)$, $0^+(3)$, 0(2), 0(3), 1(3), 1(4), 1(5), 2(2), 2(3), 3(1)	120	112
$Al(^2P_{1/2u})$+$Cl(^2P_{1/2u})$	$0^+(4)$, 0(4), 1(6)	875	882
$Al(^2P_{3/2u})$+$Cl(^2P_{1/2u})$	$0^+(5)$, 0(5), 1(7), 1(8), 2(4)	928	994
$Al^+(^1S_{0g})$+$Cl^-(^1S_{0g})$	$0^+(6)$	19354	19109

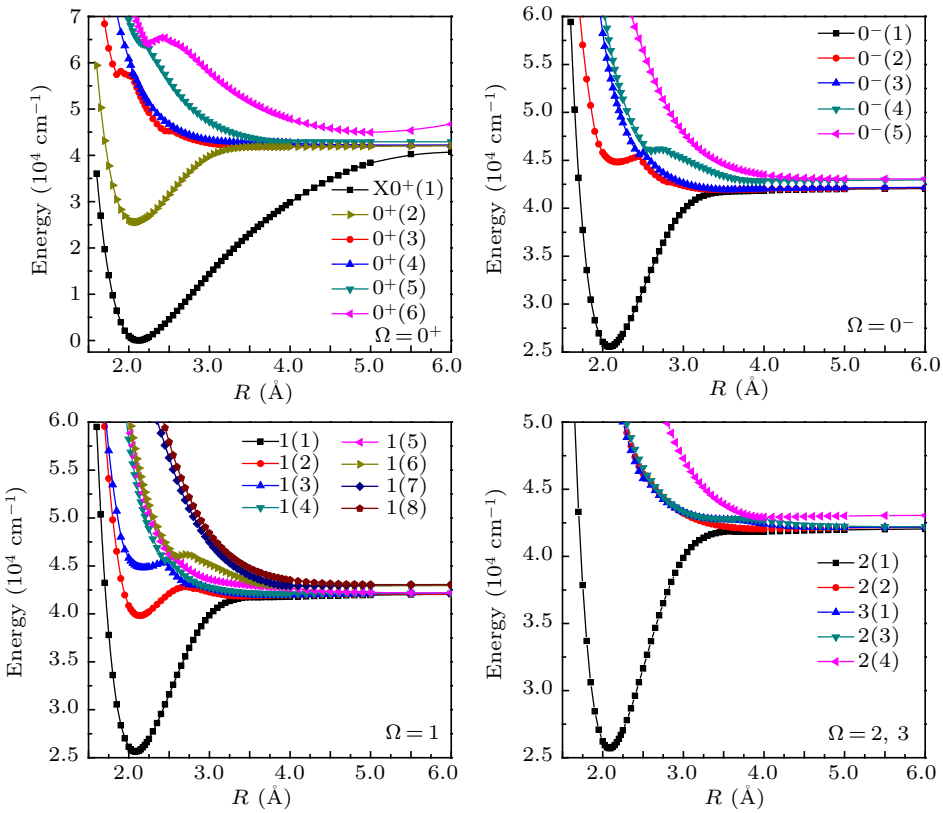


Fig. 4. PECs of a total of 24 Ω states.

Based on our calculations, the spectroscopic constants of the bound states are computed and the results are listed in Table 5. From Fig. 4, we can see that the state $X0^+$ is almost completely derived from the Λ–S state $X^1\Sigma^+$. Therefore, the spectroscopic constants are also close to those of the $X^1\Sigma^+$ state. By comparison, it can be obtained that the D_e of $X^1\Sigma^+$ state is 0.505 eV higher than that of $X0^+$ state. After considering the influence of SOC, the $a^3\Pi$ state splits into four states ($0^+(2)$, $0^-(1)$, 1(1), and 2(1)), which have deep potential wells of 16260 cm^{-1}, 15901 cm^{-1}, 15834 cm^{-1}, and 16246 cm^{-1},

respectively. Comparing with the $a^3\Pi$ state, the R_e values of these four Ω states are shortened. However, the T_e values of the four Ω states are larger than those of the corresponding Λ–S state. As can be seen from Table 5, only four states $X0^+$, $0^+(2)$, 1(1), and 2(1) are observed experimentally. Our results are in good agreement with the available experimental and previous theoretical values.[3,7,10,12,31,33] However, there is no experimental value for the vibration constant $\omega_e x_e$. So far, the $0^-(1)$ and 1(2) states have not been observed in experiment.

As shown in Fig. 5, the Λ–S components of the (1)1, (1)2, (0)1, and (2)1 states are complex. With the change of R, the Λ–S components of 1(1) state gradually become a mixture of $2^3\Pi$, $b^3\Sigma^+$, $2^3\Sigma^+$, $1^1\Sigma^-$, $1^1\Delta$, and $a^3\Pi$ states. Besides, the Λ–S component of the 1(2) state is the mixture of $A^1\Pi$, $2^3\Sigma^+$, $1^3\Delta$, $a^3\Pi$, $2^1\Pi$, and $b^3\Sigma^+$ states in a range of $R = 3$ Å–4.5 Å. From Fig. 5, we can see that the Λ–S components of these states have a complex mixture at the internuclear distance range from 2.5 Å to 4.5 Å, which indicates that there are complex SOC interactions between these Λ–S states. And the position where the composition suddenly changes corresponds to the avoided crossing points of the PECs (see Fig. 3).

Table 5. Computed spectroscopic constants of Ω states of AlCl.

State	Reference	T_e (cm^{-1})	R_e (Å)	ω_e (cm^{-1})	$\omega_e x_e$ (cm^{-1})	B_e (cm^{-1})	D_e (eV)
$X0^+$	this work		2.1205	491.20	2.2838	0.2461	5.4
	Calc.[3]		2.1374	478.13		0.2408	5.21
	Expt.[25]		2.130	481.7	2.0700	0.2439	5.25±0.01
$0^+(2)$	this work	25552	2.0847	523.9	2.4242	0.2548	2.6
	Calc.[3]	23905	2.1049	525.82		0.2484	2.29
	Expt.[7]	24528	2.1000	524.35		0.250	
	Expt.[31]	24793				0.2501	
$0^-(1)$	this work	25552	2.0847	523.80	2.4117	0.2548	2.01
	Calc.[3]	23905	2.1049	525.82		0.2484	2.25
1(1)	this work	25623	2.0838	523.6	2.4264	0.2548	1.98
	Calc.[3]	23960	2.1050	525.68		0.2483	2.24
	Expt.[7]	24594	2.1000	524.35		0.250	
	Expt.[31]	24855				0.2518	
2(1)	this work	25552	2.0847	523.9	2.4242	0.2548	2.06
	Calc.[3]	24015	2.1050	525.55		0.2483	2.25
	Expt.[7]	24658	2.1000	524.35		0.250	
	Expt.[31]	24920				0.2535	
1(2)	this work	39812	2.1364	443.00	10.2524	0.2427	0.28
	Calc.[3]	38224	2.1330	455.60		0.2408	0.54

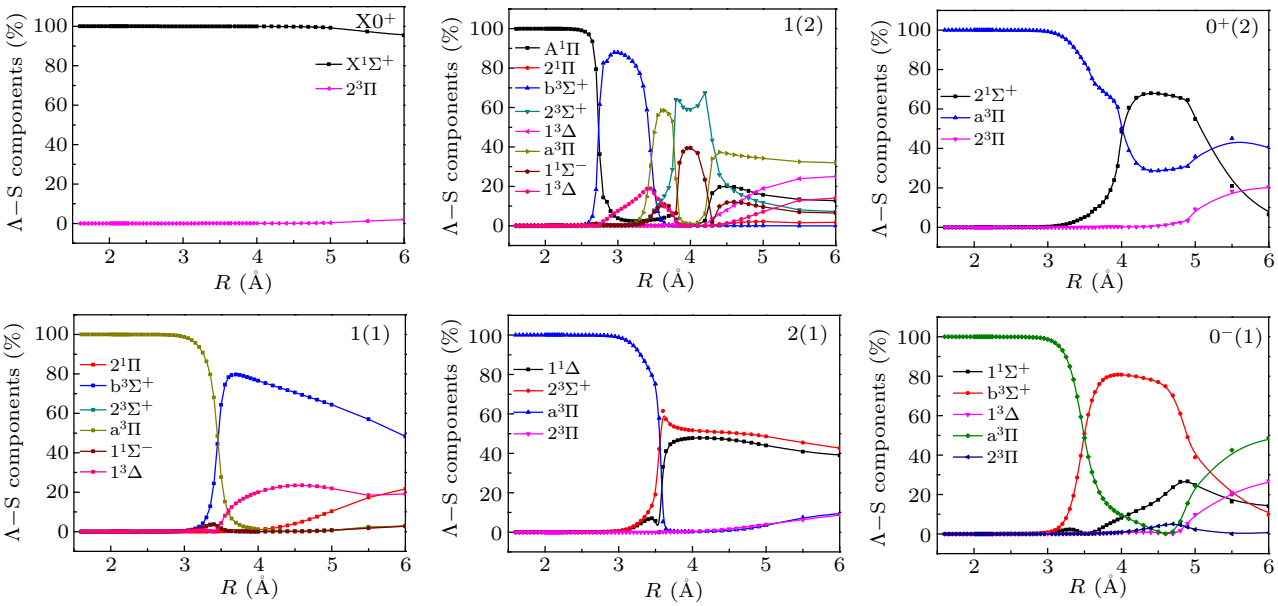


Fig. 5. Curves of Λ–S component of $X0^+$, $0^-(1)$, $0^+(2)$, 1(1), (1)2, and 1(2) states.

3.4. TDMs, FCFs, and raiative lifetimes of AlCl molecule

The transition dipole moments containing 1(1)–X0$^+$, 1(2)–X0$^+$, and 0$^+$(2)–X0$^+$ are calculated each as a function of R in a range from 1.9 Å to 8 Å. The corresponding TDM curves are shown in Fig. 6.

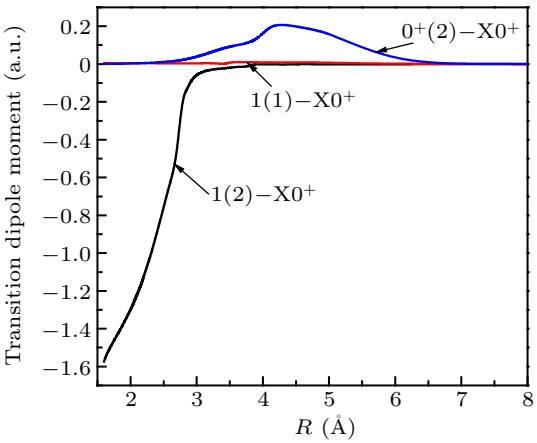


Fig. 6. Transition dipole moments of AlCl.

It is obvious from the figure that the absolute TDM value of the 1(2)–X0$^+$transition is much larger than the absolute TDM values of 1(1)–X0$^+$ and 0$^+$(2)–X0$^+$ in the Franck–Condon region. The main reason is that the 1(2)–X0$^+$ transition comes mainly from the spin-allowed transition A$^1\Pi$–X$^1\Sigma^+$, while the transitions 0$^+$(2)–X0$^+$ and 1(1)–X0$^+$ come from the spin-forbidden transition a$^3\Pi$–X$^1\Sigma^+$. It can also be seen that the TDM value of 1(2)–X0$^+$ decreases rapidly with the increase of R, which is due to the fact that the Λ–S components of 1(2) state changes from A$^1\Pi$ state to other triple states near $R = 3.2$ Å.

The FCFs of the 0$^+$(2)–X0$^+$, 1(1)–X0$^+$, and 1(2)–X0$^+$ transitions are calculated with the help of the LEVEL program,[34] and the results are displayed in Table 6. With the calculations of TDMs and FCFs, we calculate the radiative lifetime τ of the vibration level v' at a specified state, which is calculated from the following formula:

$$\begin{aligned}\tau_{v'} &= (A_{v'})^{-1} \\ &= \frac{3h}{64\pi^4 |a_0 \times e \times \mathrm{TDM}|^2 \left(\sum_{v''} q_{v',v''} (\Delta E_{v',v''})^3\right)} \\ &= \frac{4.936 \times 10^5}{|\mathrm{TDM}|^2 \sum_{v''} q_{v',v''} (\Delta E_{v',v''})^3},\end{aligned}$$

where TDM (in atomic unit) is the average electronic transition dipole moment, $q_{v'v''}$ is the Frank–Condon factor of the two vibration levels, $\Delta E_{v'v''}$ is the energy difference in units of cm^{-1}.

The results of the radiative lifetime and the reference experimental values are listed in Table 7. The radiative lifetime of 1(2)–X0$^+$ is much longer than that of 0$^+$(2)–X0$^+$ and 1(1)–X0$^+$. The radiative lifetime for 1(2)–X0$^+$ is in unit of ns, and the other two are in unit of ms. Among them, the radiative lifetime of 0$^+$(2)–X0$^+$ calculated by us has a certain gap with the theoretical value.[3] The reason is that the lifetime of spin-forbidden 0$^+$(2)(a$^3\Pi_{0+}$)–X$^1\Sigma^+_{0+}$ arises mainly from the spin–orbit couplings. In Ref. [3], only three Λ–S states, X$^1\Sigma^+$, a$^3\Pi$, and X$^1\Pi$ are included in the SOC computations. While our

Table 6. Franck–Condon factors of selected transitions for AlCl.

	Reference	$v''=0$	$v''=1$	$v''=2$	$v''=3$	$v''=4$	$v''=5$	$v''=6$	$v''=7$	$v''=8$
						0$^+$(2)-X0$^+$				
$v'=0$	this work	0.855804	0.129889	0.013060	0.001139	0.000097	0.000009	0.000001	0.000000	0.000000
	Calc.[3]	0.8812	0.1103	0.0080	0.0004					
$v'=1$		0.136014	0.607856	0.216385	0.034929	0.004255	0.000478	0.000062	0.000012	0.000004
	Calc.[3]	0.1121	0.6678	0.1955	0.0229					
$v'=2$		0.007961	0.238845	0.411455	0.268017	0.061740	0.010089	0.001521	0.000263	0.000065
$v'=3$		0.000218	0.022507	0.313310	0.257119	0.290532	0.091785	0.019534	0.003799	0.000828
						1(1)-X0$^+$				
$v'=0$	this work	0.856791	0.129053	0.012927	0.001124	0.000095	0.000009	0.000001	0.000000	0.000000
	Calc.[3]	0.8816	0.1100	0.0080	0.0080					
$v'=1$		0.135203	0.610535	0.215004	0.034507	0.004197	0.000472	0.000061	0.000013	0.000004
	Calc.[3]	0.1117	0.6690	0.1949	0.0227					
$v'=2$		0.007796	0.237457	0.414949	0.266860	0.061092	0.009970	0.001509	0.000260	0.000064
$v'=3$		0.000208	0.022086	0.312170	0.260555	0.289831	0.090961	0.019263	0.003739	0.000820
						1(2)-X0$^+$				
$v'=0$	this work	0.963348	0.033065	0.003348	0.000223	0.000015	0.000001	0.000000	0.000000	0.000000
	Calc.[3]	0.9988	0.0005	0.0007	0.000000					
$v'=1$	this work	0.036574	0.861475	0.086446	0.013907	0.001441	0.000141	0.000014	0.000002	0.000000
	Calc.[3]	0.0005	0.9970	0.000109	0.0025					
$v'=2$		0.000014	0.104203	0.699812	0.152645	0.036616	0.005766	0.000825	0.000103	0.000015
$v'=3$		0.000060	0.001043	0.201694	0.484873	0.213839	0.076833	0.017510	0.003459	0.000566

Table 7. Spontaneous radiative lifetimes of AlCl molecule, with SOC coupling taken into consideration.

Transition	Unit	Radiative lifetimes						Reference
		$v'=0$	$v'=1$	$v'=2$	$v'=3$	$v'=4$	$v'=5$	
$0^+(2)$–$X0^+$	ms	1.44	1.43	1.94	1.42	1.42	1.54	this work
		39.07	41.47	43.77	45.88	47.75	49.26	Calc.[3]
$1(1)$–$X0^+$	ms	1.1	1.09	1.09	1.08	1.08	1.08	this work
		1.58	1.60	1.63	1.65	1.68	1.71	Calc.[3]
$1(2)$–$X0^+$	ns	5.48	5.52	5.57	5.62	5.69	4.5	this work
		4.99	5.13	5.29	5.47	5.68	5.93	Calc.[3]
		5.17	5.28	5.40	5.55	5.73	5.92	Calc.[9]
		5.9	6.1	6.3	6.6	6.8	7.1	Calc.[14]
		6.4±2.5						Expt.[13]

computations indicate that the $2^1\Sigma^+$ state is mixed with the $0^+(2)(a^3\Pi_{0+})$ state, since the $2^1\Sigma^+$–$X^1\Sigma^+$ is a spin-allowed transition, the mixing with $2^1\Sigma^+$ state in the $0^+(2)(a^3\Pi_{0+})$ state will shorten the lifetime of $0^+(2)(a^3\Pi_{0+})$–$X^1\Sigma^+_{0+}$. The absence of high-lying $2^1\Sigma^+$ state is the main source of difference in lifetime. The radiative lifetime τ of $1(1)$–$X0^+$ is very close to a theoretical value.[3] The radiative lifetime τ of $1(2)$–$X0^+$ is 5.48 ns, which is in agreement with experimental value of 6.4±2.5 ns.[35]

4. Conclusions

In this work, the low-lying states of the AlCl molecule are calculated by the high-level *ab-initio* MRCI-F12+Q method. We make different corrections to obtain the accurate spectroscopic constants of the three lowest electronic states of AlCl. The PECs of 13 Λ–S states are calculated, which are related to the two dissociation limits $Al(^2P_u)+Cl(^2P_u)$ and $Al^+(^1S)+Cl^-(^1S)$. On the basis of PECs, the calculated spectroscopic constants are in good agreement with the experimental values. The calculated PECs show that the $A^1\Pi$ and $a^3\Pi$ states intersect with some other excited states and the SOC coupling effect cannot be ignored. After considering the SOC effect, 13 Λ–S states split into 24 Ω states, and the two dissociation limits split into five dissociation limits. With the help of calculated SO matrix elements, the predissociation mechanism of the $A^1\Pi$ state is analyzed. The radiative lifetime τ of $1(2)$–$X0^+$ is 5.48 ns, which is in agreement with experimental value of 6.4±2.5 ns. Our work shows that the AlCl molecule has fairly accurate and detailed electronic structure and spectral information, which plays an important role in studying the electronic structure of molecule containing heavy atoms.

References

[1] Cernicharo J and Guélin M 1987 *Astron. Astrophys.* **183** L10
[2] Rosenwaks S 1976 *J. Chem. Phys.* **65** 3668
[3] Wan M J, Yuan D, Jin C G, Wang F H, Yang Y J, Yu Y and Shao J X 2016 *J. Chem. Phys.* **145** 024309
[4] Wells N and Lane I C 2011 *Phys. Chem. Chem. Phys.* **13** 19018
[5] Yang R, Tang B and Gao T 2016 *Chin. Phys. B* **25** 043101
[6] Shuman E S, Barry J F and Demille D 2010 *Nature* **467** 820
[7] Sharma D 1950 *American Astronomical Society* **113** 210
[8] Hedderich H G, Dulick M and Bernath P F 1993 *J. Chem. Phys.* **99** 8363
[9] Langhoff S R, Bauschlicher C W and Taylor P R 1988 *J. Chem. Phys.* **88** 5715
[10] Dearden D V, Johnson R D and Hudgens J W 1993 *J. Chem. Phys.* **99** 7521
[11] Saksena M D, Dixit V S and Singh M 1998 *J. Mol. Spectrosc.* **187** 1
[12] Mahieu E, Dubqis I and Bredohl H 1989 *J. Mol. Spectrosc.* **134** 317
[13] Rogowsiu D F and Fontijn A 1987 *Chem. Phys. Lett.* **137** 219
[14] Brites D H V and Hochlaf M 2008 *J. Phys. Chem. A* **112** 13419
[15] Yousefi M and Bernath P F 2018 *The Astrophysical Journal Supplement Series* **237** 8
[16] Werner H J, Knowles P J, Knizia G, Manby F R and Schütz M 2012 *Wires. Comput. Mol. Sci.* **2** 242
[17] Werner H J and Knowles P J 1985 *J. Chem. Phys.* **82** 5053
[18] Werner H J and Meyer W 1980 *J. Chem. Phys.* **73** 2342
[19] Langhoff S R and Davidson E R 1974 *Int. J. Quantum Chem.* **8** 61
[20] Douglas M and Kroll N M 1974 *Ann. Phys.* **82** 89
[21] Peng D and Hirao K 2009 *J. Chem. Phys.* **130** 044102
[22] Reiher M and Wolf A 2004 *J. Chem. Phys.* **121** 10945
[23] Pitzer R M and Winter N W 1988 *J. Phys. Chem.* **92** 3061
[24] Tilson J L and Ermler W C 2014 *Theoretical Chemistry Accounts* **133** 1564
[25] Wyse F C and Gordy W 1972 *J. Chem. Phys.* **56** 2130
[26] Jastrzebski W, Kowalczyk P, Szczepkowski J, Allouche A R, Crozet P and Ross A J 2015 *J. Chem. Phys.* **113** 2116
[27] Martin W C and Zalubas R 1979 *J. Phys. Chem. Ref. Data* **8** 817
[28] Radziemski L J 1969 *J. Opt. Soc. Am.* **59** 424
[29] Radziemski J, Leon J and Kaufman V 1974 *J. Opt. Soc. Am.* **64** 366
[30] Huber K P and Herzberg G 1979 *Molecular Spectra and Molecular Structure IV. Constants of Diatomic Molecules* (New York: Van Nostrand Reinhold)
[31] Ram R S, Rai S B, Upadhya K N and Rai D K 1982 *Phys. Scr.* **26** 383
[32] Hildenbrand D L and Theard L P 1969 *J. Chem. Phys.* **50** 5350
[33] Kumar Y, Khanna B N and Varshney D C 1985 *Indian J. Pure Appl. Phys* **23** 128
[34] Le Roy R J 2017 *J. Quantum Spectrosc. Radiat. Transfer* **186** 167–168
[35] Mahieu E, Dubois I and Bredohl H 1989 *H. J. Mol. Spectrosc.* **138** 264